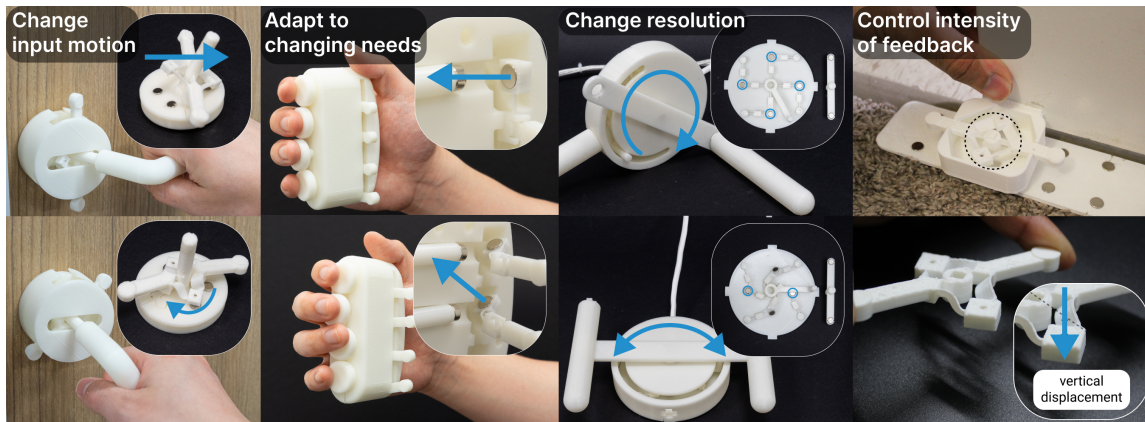


1 Reconfigurable Interfaces by Shape Change and Embedded Magnets

2
3 ANONYMOUS AUTHOR(S)*
4



20
21 Fig. 1. Our approach enables easy reconfiguration of physical interfaces in the form of input motions, adapting to changing needs,
22 changing the resolution of the interface, and feedback intensity through shape change and displacement of embedded magnets.

23 Reconfigurable physical interfaces empower users to swiftly adapt them to tailor design requirements or preferences. Shape-changing
24 interfaces enable such reconfigurability, avoiding the cost of refabrication or replacements of parts. Nonetheless, reconfigurable
25 interfaces are often bulky, expensive, or inaccessible. We propose a reversible shape-changing mechanism that enables reconfigurable
26 3D printed structures via translations and rotations of parts. We investigate fabrication techniques that allow the reconfiguring of
27 interfaces using magnets and the thermoplastic nature of heated polymer. Proposed tangible interfaces achieve fine-tunable haptic
28 feedback and adjustment of different user affordances by reconfiguring input motions. We present a design space and demonstrate it
29 through applications in rehabilitation, embodied communication, accessibility, safety, and gaming.
30

31
32 CCS Concepts: • Human-centered computing → Human computer interaction (HCI).

33 Additional Key Words and Phrases: Shape Change, Magnets, Fabrication

35 ACM Reference Format:

36 Anonymous Author(s). 2018. Reconfigurable Interfaces by Shape Change and Embedded Magnets. In *Woodstock '18: ACM Symposium*
37 *on Neural Gaze Detection, June 03–05, 2018, Woodstock, NY*. ACM, New York, NY, USA, 19 pages. <https://doi.org/XXXXXX.XXXXXXX>

40 1 INTRODUCTION

41 In the rapidly evolving technological landscape, the demand for adaptable and personalized physical interfaces has
42 grown substantially. While many modern digitization of input and output has displaced physical interfaces, they
43 provide embodied interaction for non-visual information, multi-modal feedback for interactions in virtual reality (VR),
44

45 Permission to make digital or hard copies of all or part of this work for personal or classroom use is granted without fee provided that copies are not
46 made or distributed for profit or commercial advantage and that copies bear this notice and the full citation on the first page. Copyrights for components
47 of this work owned by others than ACM must be honored. Abstracting with credit is permitted. To copy otherwise, or republish, to post on servers or to
48 redistribute to lists, requires prior specific permission and/or a fee. Request permissions from permissions@acm.org.

49 © 2018 Association for Computing Machinery.

50 Manuscript submitted to ACM

and also partly contribute to the field of accessibility by simulating different human capabilities from what has been impaired. Yet, traditional interfaces often require costly refabrication or part replacements to accommodate changing user preferences, and requirements [8, 25, 26], posing significant challenges in terms of cost, time, and sustainability as also noticed in prior works [36, 37]. Shape-changing interfaces offer an innovative solution to this problem by enabling mechanical reconfigurability without the need for extensive manufacturing processes. These include a variety of physical reconfigurable devices, like input knobs [9], linear interfaces with rich input and output capabilities[19, 20], and pin-arrays [5]. Despite their potential, however, creating these interfaces remains challenging due to bulkiness, production cost, and accessibility.

In response, previous works explored fabrication techniques that leverage the intrinsic material properties of heated 3D printed thermoplastic (e.g., PLA: PolyLactic Acid) [1, 29, 31, 32]—expansions and contractions due to external heat trigger [11], many equipped into novel actuators [6, 10, 11]. Despite these advantages, shape-changing transformation inaccuracies introduced by printing strongly affect the usability and practical applicability. Our research explores a new fabrication technique that leverages magnets and a shape-memory thermoplastic to create a reversible shape-changing mechanism for reconfigurable interfaces. We use geometric control to constrain and guide the movements of heated thermoplastic along specified directions or rotations when force is applied, resulting in precise re-alignments of the 3D structure. As the embedded magnets move with the changed shape, the adjusted structure affects the magnetic field they exert. Utilizing these capabilities, our interfaces can be used to deliver precise haptic feedback or can afford a variety of input motions. We delve into the behavior of these structures when exposed to heat in conjunction with the embedded magnets, introducing a comprehensive design space and applications that illustrate its practical usage in rehabilitation, communication, accessibility, safety, and gaming. In sum, we contribute:

- The design of a geometrical module as a reconfigurability building block, with control parameters for a programmable displacement of embedded magnets.
- A principle for interaction reconfiguration described by the relationship of shape change and magnets that are displaced, and fabrication supports for reconfiguration.
- Exemplary applications of reconfigurable interfaces demonstrating mechanisms in various design contexts.

2 BACKGROUND AND MOTIVATION

2.1 Multi-Use Physical Interfaces

Adjusting and customizing the interaction to suit individual preferences and needs are the major benefits of reconfigurability in physical interfaces. *KnobSlider* [9] introduces an interactive physical interface that mechanically changes its shape from rotary to linear slider to adapt to various software applications. *Button+* [27] is a context-aware interface that appears and disappears based on the user’s situation to interact. Another line of work uses a series of actuators to imbibe tunability into the interface. For example, *inForm* [5] introduces a pin-array display that changes its shape, providing various interaction affordances to the user with a single display. Similarly, *LineForm* [20] also uses several actuators in series to demonstrate how a chained linear interface can shape-change and adapt to interactions such as deformation, touch, and pinch. These works show how reconfigurability is vital to enrich user interaction in physical and virtual environments. However, these systems are often bulky due to embedded actuators, and not accessible to lay users as they come with specific form-factor that do not fit bespoke interactive tangible interfaces.

We build upon the research in the realm of reconfiguring and customizing 3D printed tangible objects. For instance, *Reconfig*[35] combines compliant mechanism and tensioning cables to develop a multi-modal kinematic mechanism

105 capable of dynamically altering their degree of freedom. Another research direction involves enhancing and customizing
106 existing physical objects. *Reprise* [3] creates 3D printed structures that allow users to modify everyday objects for a
107 specific type of action, such as adapting a wire cutter for single-finger operation. Work by Davidoff et al. [4] and Li
108 et al. [13] involves 3D printed add-on mechanism to actuate static objects such as adjusting the angle of a desk lamp
109 [13], turning a car's climate control dial [4], or remotely silencing an alarm clock [24], showing the significance of
110 customizing and reconfiguring tangible interfaces. However, a persistent challenge is the (re)fabrication of these add-on
111 mechanisms, which require external electro-mechanical actuators, microprocessors, and software coding.
112
113

114

115

2.2 Adaptive 3D printed Objects using Shape-changing

116

117 Researchers have approached 3D printing shape-changing interfaces to achieve complex linear 3D structures from sticks
118 printed flat [31], transforming them by shifting directions of stimulus [28], and more. Combining shape-changeable
119 objects with other materials such as TPU [1], carbon-composite PLA [18], and copper-sheet [23] activate transformation
120 to obtain desired behaviors. For instance, chemically dissimilar bilayer structures release residual stress to bend a
121 sample (e.g., [1]). *ShrinkCells* [18] and *Exoform* [23] use conductive materials either 3D printed or attached later on to
122 control the activation time and to reconfigure the original shape per context, such as nailing the hook in and taking
123 it out [18]. Although combining various materials in 3D printing allows for versatile activation of deformation, the
124 generated shape changes are primarily limited to alterations in form factor [1, 18, 31]. Unfortunately, the force exerted
125 by these shape shifts is insufficient to offer reconfigurability. To broaden the application of shape-changing objects in
126 delivering haptic feedback and reshaping interaction affordances, we incorporate neodymium magnets within the 3D
127 printed thermoplastic structures. This enhances the force feedback substantially, going beyond the limited residual
128 force inherent in PLA filaments.
129
130

131

132

133

2.3 Magnets in Tangible Interfaces

134

135 Permanent magnets (e.g., neodymium magnets) often provide kinesthetic haptic feedback through pulling/pushing
136 forces arranged by polarity, position, and intensity. Several works introduced embedding magnets to interact with
137 tabletop or portable displays [2, 14, 15, 33]. *Madgeit* [33] shows embedded passive magnets enabling physical interface
138 to move, vibrate and power touch displays. With magnet-induced forces, users can create interactive drawings [14] with
139 tangible blocks and identify different objects [15] with variable magnetic force. These interactions, however, are limited
140 to 2D screens and require multiple physical interfaces with different topologies to attain more than one interaction (e.g.,
141 rotating and pushing), or changing the slider intervals, from discrete to continuous. Beyond 2D interface, *MagnetIO* [16]
142 introduced a soft stretchable magnetic patch that can be attached to a body and everyday objects on various surfaces,
143 enabling them to provide vibrotactile feedback when touched with a wearable device. *Mechamagnets* [36] introduced a
144 tangible interface that facilitates permanent magnets with various topologies to provide kinesthetic feedback in various
145 forms, such as linear, planar, polar, radial, and angular motions. *Magneto haptics* [21], *Magnetips* [17], and *Omni* [12]
146 have leveraged magnetism to enable both tracking and haptic feedback through embedding permanent magnets in
147 tangible interfaces. Our work also provides kinesthetic feedback with permanent magnets in various orientations,
148 positions, and intensities but most importantly, within a single 3D printed shape-changing interface that does not
149 require external electromagnet to provide haptic feedback, yet still can afford different interaction styles from rotation
150 to linear on the one hand, catering different extents of forces.
151
152

153

154

155

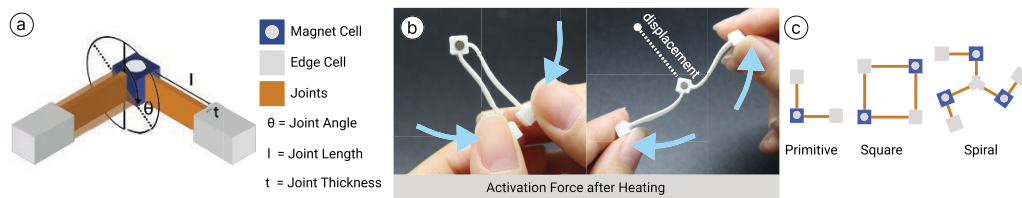
157 3 RECONFIGURABILITY PRIMITIVE: PRINCIPLES AND DESIGN OF BUILDING BLOCK

158 **Thermoplastic Behavior.** Thermoplastics become flexible when heated and respond to external activation and
 159 deactivation forces for shape change. Among them, polymers such as PLA present shape memory properties, such
 160 that once deformed under heat, they revert to the original state just by re-applying the heat as an activation trigger.
 161 Such shape change only requires activation force while retention of the changed shape and reversion to the original
 162 shape happen through thermoplastic and shape memory properties. However, this shape change is unpredictable in
 163 its repeatability as it is heavily human-dependent on how external forces are applied. However, prior work [7, 22]
 164 has shown how geometric control can be leveraged for predictable and repeated shape change even when the shape
 165 changing forces are applied by humans. We take inspiration from these works to control the geometry of our structures
 166 and constrain the areas of force application to ensure predictable repeatability.
 167

168 **Planning Predictable Deformations through Geometry Control.** As introduced in prior work, square cells can
 169 shear, bend, and twist when aligned based on the angles of the opposing flexible hinges determining the in-plane or
 170 out-of-plane shape change [22]. The same principle applies to heat-based shape change by designing the geometry
 171 of a modular primitive. Intuitively, the malleability achieved after heating PLA is affected by the printed thickness
 172 and length. Longer and thinner parts heat up faster and bend easily due to the overall surface area heated directly,
 173 whereas, thicker parts take longer to heat throughout. Furthermore, the closer the length gets to the thickness, these
 174 parts become more difficult to bend. Using this logic, we devise the shape-change geometry with specific cells for force
 175 application, magnet housing, and hinge behavior.
 176

177 3.1 Primitive Design

178 **In/out-of-plane Displacement to Reconfigure Magnetic Fields.** In this work, we are specifically interested in the
 179 in-plane and out-of-plane displacement of magnets embedded in the printed geometry which is a result of the applied
 180 shape change. The geometry is designed in such a way that the displacement of the sections experiencing propagated
 181 force can be controlled through parametric constraints and these sections can hence house the embedded magnet. The
 182 shape change geometry is extracted from an elbow joint which leverages the displacement of “edge cells” to cause
 183 displacement in the “magnet cell” through the control of “joint angle”, and “joint length” as highlighted in Figure 2(a).
 184



185 Fig. 2. The structure of the shape-change geometry (a) is extracted from an elbow-joint building block: magnet cell, joints, and edge
 186 cells. Geometric parameters program displacement of the magnet cell through shape change. Activation forces (b) are applied at the
 187 edge cells to bring them closer, or pull them apart in the same plane. We explore three topologies of the primitive (c).
 188

- 189
- 190 • **Joints:** We design joints to be the thinnest and longest parts of the geometry so that they easily change shape on
 191 application of heat and activation forces. These joints, hence, act as hinges for the rest of the structure.
 - 192 • **Edge Cells:** These are the parts where manual activation force is applied. The force is applied along an arc connecting
 193 the cells. We design the edge cells to have a thickness to length ratio closer to 1, i.e. on application of heat and force,
 194 they will heat up but will not easily bend, propagating the force to the adjoining joints.

- 209 • **Magnet Cell:** It is the part that is displaced in or out of its plane when activation force is applied to the edge cells in
 210 particular directions. It is designed as a cuboid with a hole where a magnet is inserted, and does not change its shape
 211 (thickness to length ratio close to 1). It moves in the 3D space by having forces propagated from edge cells through
 212 adjoining joints displacing the magnet cell and changing the resultant magnetic field of the embedded magnet with
 213 respect to its original position.
 214

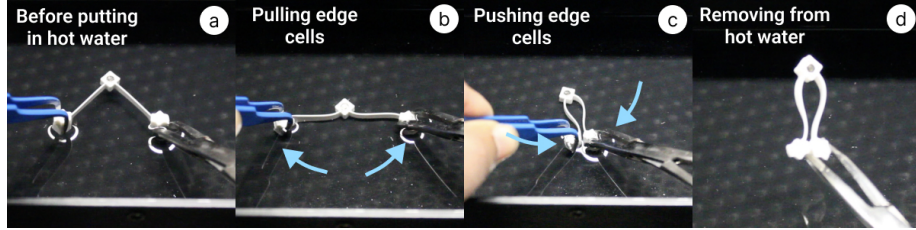


Fig. 3. Process of triggering reconfiguration in hot water

225 **Triggering Reconfiguration.** We first heat the geometry using hot water, to apply heat uniformly as approached
 226 in many prior works. Note that in an end-user scenario, a more sophisticated embedded heating mechanism may be
 227 considered, including nichrome wires and/or conductive filaments for selective and sequential heating as needed. Once
 228 heated, pushing or pulling force is applied to the edge cells of the primitive geometry in a single arc connecting the two
 229 edge cells (Figure 2(b), Figure 3). This manual force is propagated through the joints to the magnet cell, and depending
 230 on the joint angle and length, displacement of the magnet cell from its original position can be predicted. We explore
 231 three topologies of the primitive i.e. the primitive, square, and the spiral arrangement of module (Figure 2(c)).
 232

3.2 Displacement Modules and Control Parameters

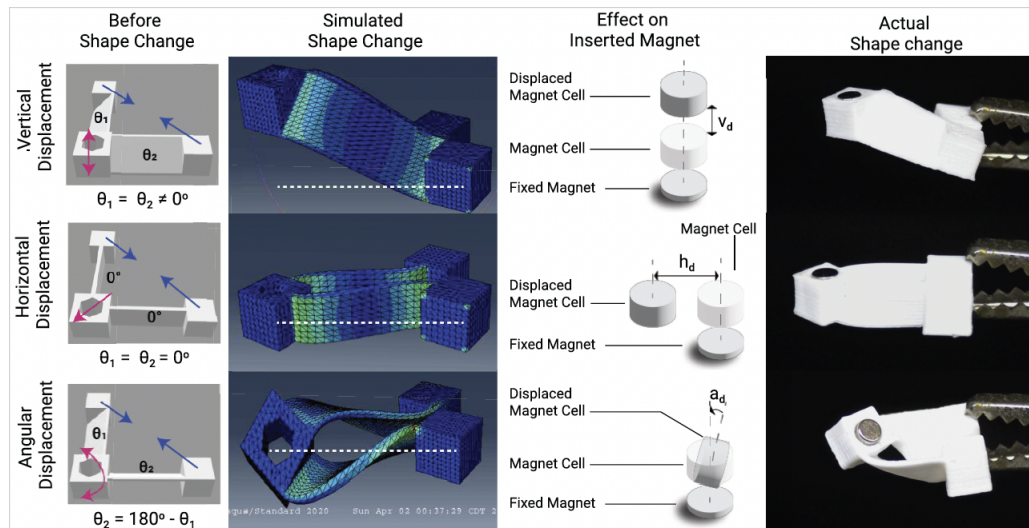


Fig. 4. Vertical, Horizontal, and Angular displacement modules before and after shape change with their simulated models and the abstraction of the effect on embedded magnets.

Considering a fixed magnet directly below the magnet cell, displacing the magnet cell would change the attraction forces between the two magnets. If the magnet cell displaces beyond a certain distance or angle, the attraction forces will not affect the fixed magnet and the magnet cell, similar to “deactivating” the magnet cell. We can hence use the displacement modules (Figure 4) to affect the two magnets’ magnetic field through predetermined shape change.

- **Vertical Displacement Module:** Vertical displacement (v_d) of the magnet cell is its displacement along the Z axis. Empirically, we found that the magnet cell is displaced vertically along the Z axis when both the adjoining joint angles are equal ($\theta_1 = \theta_2$).
- **Horizontal Displacement Module:** Horizontal displacement (h_d) of the magnet cell is seen when the joints are printed at 0° . This displacement is in the same plane as the magnet cell’s previous position i.e. the X-Y plane. The direction of applied force to the edge cells determines the direction of the horizontal displacement.
- **Angular Displacement Module:** Angular displacement (a_d) of the magnet cell is the twisting of the magnet’s orientation with respect to the X-Y plane. When the joint angles are opposite ($\theta_1 = 180^\circ - \theta_2$), the magnet cell twists in an angular displacement.

3.3 Fabricating Reconfiguration Supports for End User Actions

We have explored a few of the possible topologies as can be seen from Figure 2 (c). While each topology provides reconfigurability, from the end-user perspective, the input to cause shape change can become difficult when multiple edge cells are involved. A designer may want to hide the inner mechanism from the end user, but it would be imperative to provide access to reconfigure the mechanism in a quick and easy fashion. We explored additional supports for the mechanisms such that more than one magnet cell might be shape changed at once depending on the topology without knowing the inner workings.

Push/Pull Edge Cells. For a simple primitive topology or even a square topology (Figure 2 (c)), an end user may have access to the edge cells to push them apart or closer together. However, considerations need to be made when exposing multiple edge cells to the end user for displacing multiple magnet cells.

Rotate Pole to Reshape. To make it easier to change shape with one swift motion correctly, we can add a central pole that connects the edge cells, such that, rotating the pole would cause the edge cells to move closer to each other. This makes sure that the center of shape change is preserved and no unnecessary displacement of the magnet cell is caused by human error (Figures 5 and 6). The addition of the central pole also enables simultaneous displacement of multiple magnet cells. For the square topology (Figure 2 (c)), we connect the edge cells to the center pole with thin printed connectors. We add stoppers at the base of the edge cells to prevent them from rotating. Hence, on rotation of the center pole, as rotation of edge cells is blocked, they move closer to the pole with the thin connectors twisting around the pole (Figure 5).

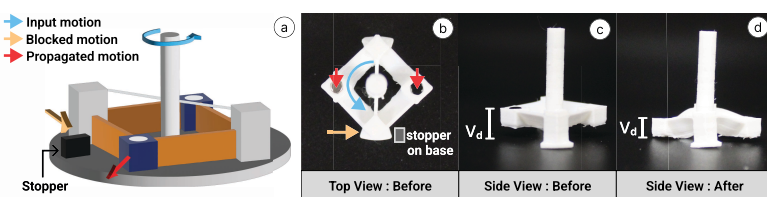


Fig. 5. A square topology can utilize a center pole with thin connectors from the edge cells to the pole, and stoppers at the base (a,b,c) such that rotating the center pole would result in pushing the two edge cells together causing magnet cell displacement (d)

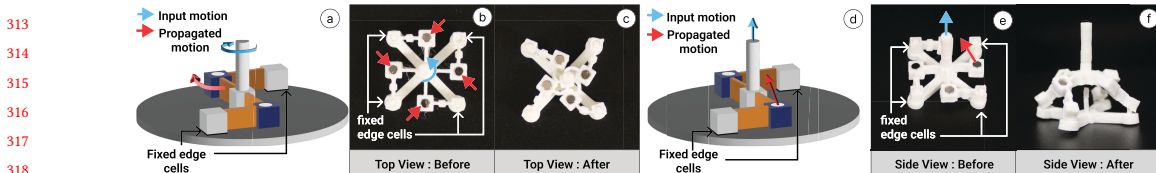


Fig. 6. A spiral topology can also utilize a center pole and stoppers, but it can also have its edge cells fixed (a,b). The rotation of the pole would result in magnets cells moving closer to the pole (c), and pulling up the pole (d,e) would result in a dome shape (f)

For the spiral topology (Figure 7), the central pole sits at the spiral's center. Here, two possible configurations are possible. First, where the central pole connects the edge cells similar to Figure 5 with stoppers. Second, we can fix the outer edge cells of the spiral and simply rotate the central pole in clockwise or anticlockwise direction to move the magnet cells closer or further away from the center (Figure 6 (d)).

Pull Pole to Reshape. Beyond rotating the center pole, if the edge cells are fixed, an end user can also pull up the pole. This would be equivalent to pulling apart the edge cells but in a slanted plane (Figure 6(e)). The displacement can then be predicted with respect to the slanted plane. While more complicated topologies and placements of the central pole may be possible, these simpler topologies can serve as building blocks.

4 DESIGN OF RECONFIGURABLE INTERFACES BY SHAPE CHANGE AND EMBEDDED MAGNETS

In order to design complete interfaces utilizing the working principle of the primitive, we propose a design space of options available to designers. Our proposed design space includes ways to control the displacement of embedded magnets through shape change, options for topologies, support for end users to reconfigure the interfaces easily, and the available interface properties that can be reconfigured. We now describe how the interfaces can be reconfigured and what properties are affected. We demonstrate accompanying applications to elaborate on the use context.

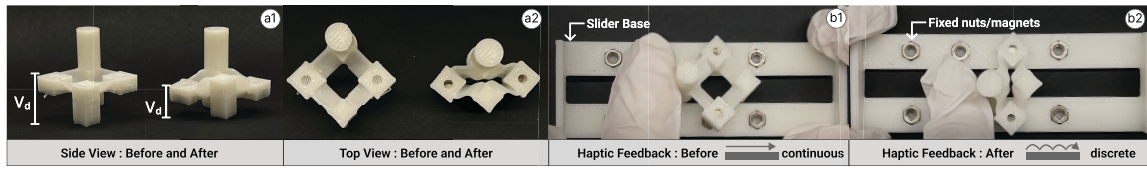
Displacement Modules	Control Parameters	Topologies	Reconfiguration Supports	Reconfiguration User Action	Reconfigured Interface Properties
Vertical	Joint Angles	Primitive Square	Center Pole Connecting Edge Cells	Rotate center pole	Haptic Feedback
Horizontal	Joint Length	Spiral	Motion Restricting Stoppers Fixed Edge Cells	Pull up center pole Push edge cells together or apart	
Angular					Input Types

Fig. 7. The design space describes the different options available to design reconfigurable interfaces as building blocks.

4.1 Reconfiguration of Interface Properties: Applications

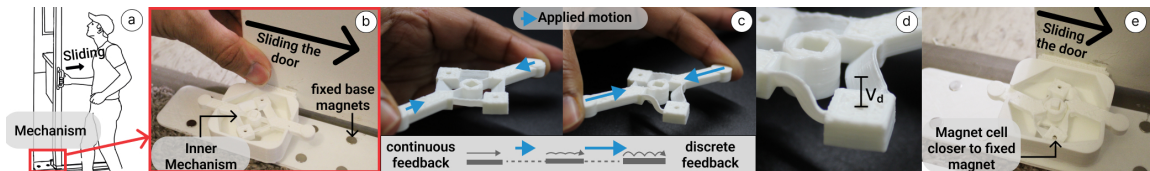
4.1.1 Haptic Feedback. By moving the magnet cells closer and further away from the fixed base magnets through vertical and horizontal displacement, or changing their orientation through angular displacement, the effect of magnetic forces can be affected resulting in changes in the haptic feedback received. Here we describe a few ways in which the haptic feedback can be reconfigured. Figure 8 (a1,a2) shows the use of the square topology and vertical displacement

365 to move the magnet cells closer to the ground. One application of this vertical displacement is a slider mechanism
 366 (Figure 8 (b1,b2)) with metal nuts fixed in the slider base (can be replaced with magnets themselves). Depending on the
 367 magnet cell's vertical displacement closer or further away from the fixed nuts, the haptic feedback felt from the slider
 368 mechanism can be changed. For detailed evaluation on the correlation between the displacement and the felt haptic
 369 force, refer to Section 5.2.
 370

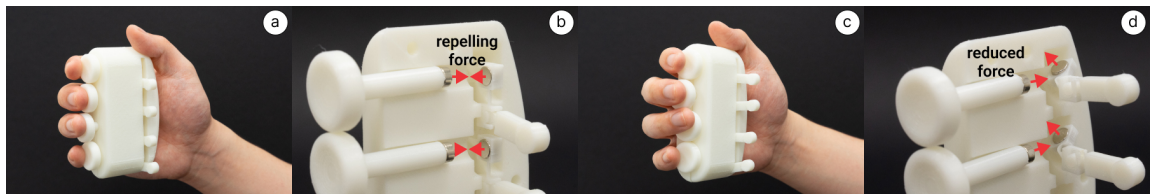


372 Fig. 8. Vertical displacement of the magnet cells moves magnets closer to the slider base (a1,a2) increasing the feedback felt while
 373 moving the slider from a continuous motion with minimal feedback to discrete stepped feedback (b1,b2).

374 **Communicating Sliding Door** Haptic feedback can be a subtle technique of communicating information. For example,
 375 if a user is conducting an important zoom call in a common workspace where multiple people are expected to show up,
 376 the user can adjust the haptic feedback of the sliding door indicating that the more force is needed to open the door, the
 377 more important it is to not make noise or disturb the user while accessing the common space. Similar to the slider in
 378 Figure 8, reconfiguring the sliding mechanism (Figure 9 (a)) to move the embedded magnets closer to the fixed magnets
 379 increases the force feedback (Figure 9 (b)).
 380



381 Fig. 9. A reconfigurable haptic attachment is connected to a sliding door with fixed magnets on the floor (a,b). When reconfigured
 382 the feedback becomes increasingly discrete (d) due to reduced distance between magnet cells and the fixed magnets (e,f).
 383

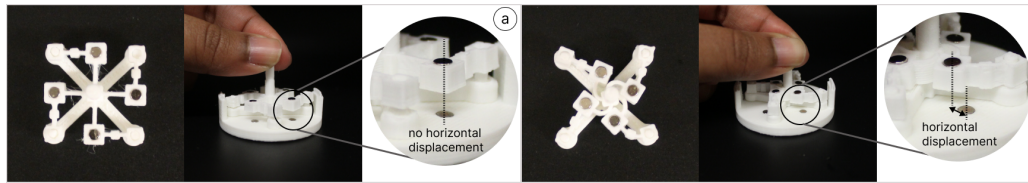


384 Fig. 10. Re-orienting the aligned magnets of a rehabilitation device (a,b) reducing force feedback (c,d).
 385

386 **Physical Rehabilitation With Grip Strengthener** We design a rehabilitation device with reconfigurable feedback
 387 where based on a user's regained grip strength, the doctor or a professional can increase the feedback force. Such a
 388 device can help adapt to changing user needs as they recover. Figure 10 shows the rehabilitation device where magnets
 389 are fixed to the buttons, and the shape changing mechanisms behind the buttons house the responding magnets. This is
 390 a direct application of the angular displacement module in Figure 4 where the primitive topology is used behind each
 391 button, and shape changing the topology results in the displacement of the embedded magnet. Two states of the device
 392

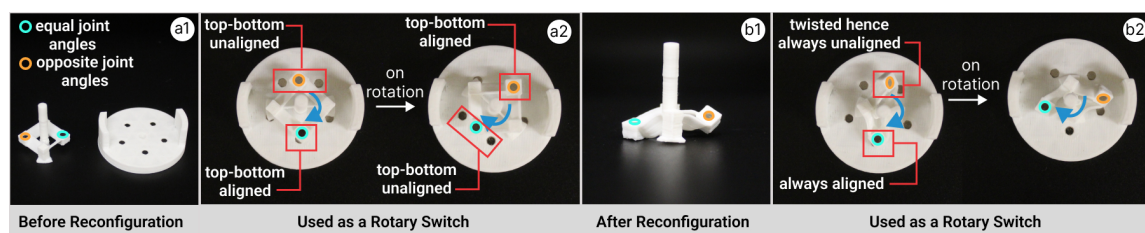
417 are shown where the magnets align exactly to provide a counterforce (Figure 10(a,b)), whereas the responding magnets
 418 undergo angular displacement to reduce their force intensity when the buttons are pressed (Figure 10(c,d)).
 419

420 Moving on to further reconfigurations in haptic feedback, we can design a rotary switch in a similar fashion where
 421 the rotation of an added center pole can move the magnet cells closer to the center, displacing them horizontally from
 422 the base magnets (Figure 11). This mechanism uses the spiral topology, and an added central pole as an end user support
 423 for reconfiguration. Twisting the pole results in applying the displacement to the magnets housed in the spiral, as
 424 described earlier about the behaviour of the pole and other supports.
 425

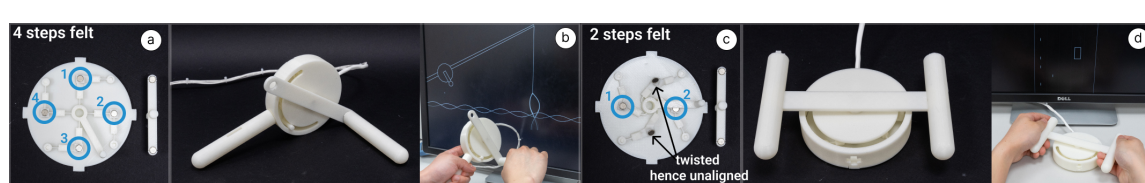


426 Fig. 11. Twisting the central pole of the spiral (a) moves all magnet cells closer to the center causing horizontal displacement (b) from
 427 the magnets fixed at the base and a change in received feedback.
 428

429 We can also modify the number of steps felt (resolution) when using an interface by activating and de-activating
 430 magnet cells through angular displacement (Figure 12). When both magnet cells of the switch using square topology
 431 are in play, a total of 10 steps are felt with using the switch (Figure 12 (a1,a2)). However, on deactivating one of the
 432 magnet cells, only 5 steps are felt (Figure 12 (b1,b2)).
 433



434 Fig. 12. The number of steps felt with two magnets in the original state of the switch (a1–a2) is reduced by half when the angular
 435 displacement module of the switch twists one magnet cell, deactivating it (b1–b2).
 436

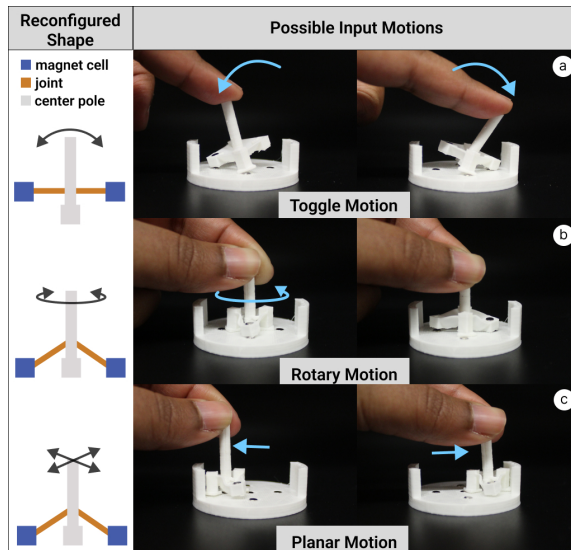


437 Fig. 13. The mechanism for the fishing rod has four steps of discrete feedback (a) felt when reeling in fish in a complete rotations.
 438 After reconfiguration, the number of steps is reduced to two (c) and felt during steering the controller to the left or right (d).
 439

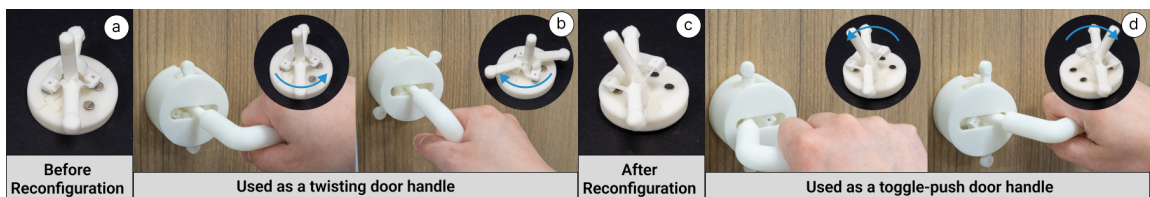
440 **Reconfigurable Game Controller** Utilizing the reconfigurable haptic feedback to modify the number of felt steps
 441 similar to Figure 12, we demonstrate a game controller design. For a fishing game, the entire rotary motion is important
 442 with feedback in the form of steps to simulate reeling in fish using a fishing rod (Figure 13 (a,b)). However, when playing
 443 a racing game, only two steps of feedback for turning left and right may be needed. In this case, we can utilize the
 444

469 angular displacement for two of the magnets in the mechanism, reducing the steps felt from four to two (Figure 13 (c)).
 470 The controller can then be used as a steering wheel using the same mechanism with a modified handle ((Figure 13 (d)).
 471

472 *4.1.2 Input Motion Affordances.* While we focus on the displacement of the magnet cell, the application of the shape
 473 change forces can result in such an overall shape that it might afford a new input motion. For example, a square topology
 474 switch as show in Figure 14(a) has space between the magnet cells and the ground such that it can pivot over a center
 475 pole for toggle motion. However, on application of a vertical displacement we can move the magnet cells close to the
 476 ground constraining the toggle motion, making it more suitable for a rotary motion Figure 14(b). Depending on the
 477 area for the switch movement and applied constraints such as a top cover for the mechanism, the rotary motion can
 478 also be turned to planar motion (Figure 14(c)).
 479



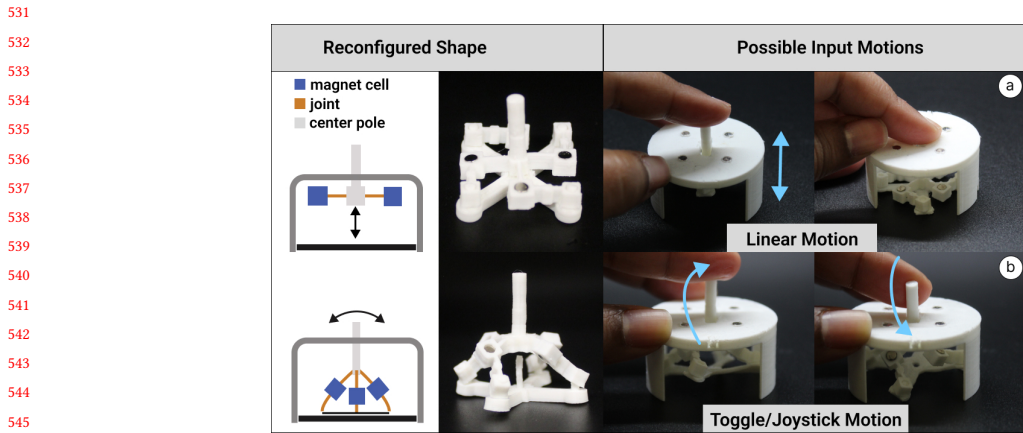
500 Fig. 14. Reconfigured shape change enables reconfiguring toggle motion (a) to rotary motion (b) to planar motion (c).



501 Fig. 15. Reconfiguring twist motion (a,b) to toggle (c,d), afforded and constrained by shape change and embedded magnets.

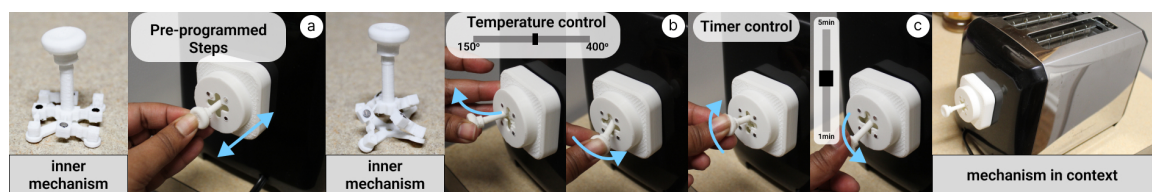
502 **Dual-Motion Door-Knob** Reconfiguring input interaction type becomes important when a design needs to cater to
 503 different types of users. Most common door knobs require a rotation/twist input to open the door. However, if a user
 504 has wrist movement issues, they will have a hard time twisting the door knob. In such a case, a door knob that can
 505 be reconfigured to be toggled open can make the interaction easy for the user. Such a door knob can hence be easily
 506 designed and printed applying our mechanism as shown in Figure 15 by reconfiguring a rotation motion (Figure 15
 507 (a,b)) to a toggle motion (Figure 15 (c,d)).
 508

521 Similarly, this manipulation of space around the mechanism can be utilized to reconfigure a push motion to a joystick
 522 motion. As seen from Figure 16, due to the space available inside the cover, it can be easily used as a push button. We
 523 place the fixed magnets in the cover. The base of the mechanism is parallel to the cover top, and when pushed, it sits
 524 flush with the ground. Due to this shape of the mechanism, the attraction to magnets in the cover prevent any toggle or
 525 joystick like motion. However, on pulling the center pole away from the base if the mechanism(Figure 6(e), a dome-like
 526 shape is created and the mechanism occupies the space in the cover restricting the push motion. It however can be used
 527 as a joystick as the magnets cells are now reconfigured on a slant, and shifting the joystick enables specific magnets to
 528 align with the fixed magnets in the cover.
 529



531 Fig. 16. Push button motion (a) can be reconfigured to a toggle or joystick motion (b) by pulling up the center pole.

532 **Supporting Different Users via Affordances** Input motion reconfiguration can help when certain functions of
 533 the device need to be made inaccessible for safety. For example, operating a toaster without knowing the extent of
 534 heat applied can be dangerous for a child without supervision or an elderly person with dementia. For users who
 535 require constrained use of the device, a simple push button can be pre-programmed with toasting settings (Figure 17(a)).
 536 However, a healthy adult may want full control over the temperature and timer settings and hence we can reconfigure
 537 the push button to a four-way toggle switch to control temperature (Figure 17(b)) and time (Figure 17(c)).



538 Fig. 17. Push interface can activate a pre-programmed set of steps for toasting (a). Reconfiguration of the mechanism can enable full
 539 control over temperature (b) and timer (c) settings through a four-way toggle motion.

540 4.2 Visual Cues to Assist End User Reconfiguration

541 A designer of these reconfigurable devices might want the user to apply a specific level of displacement to the edge cells
 542 in the form of the applied force. Given the type of the application, visual cues can be added on the fabricated widgets to

aid users in specific reconfiguration. For the three reconfiguration motions in the design space, the correlation of (1) rotating the center pole, (2) pulling it up, or (3) pushing or pulling the edge cells apart can be mapped onto a visual cue. We show an example of what such fabricated widgets might look like. Depending on the heating technique used, the materials of the widgets might need to be modified, for example, if putting the whole mechanism in hot water, the widget should be made of a material such as PolyEthylene Terephthalate Glycol (PETG, $T_g = 85^\circ\text{C}$) and Acrylonitrile Butadiene Styrene(ABS, $T_g = 105^\circ\text{C}$), with higher T_g than PLA (60°C), so that the widget itself does not deform.

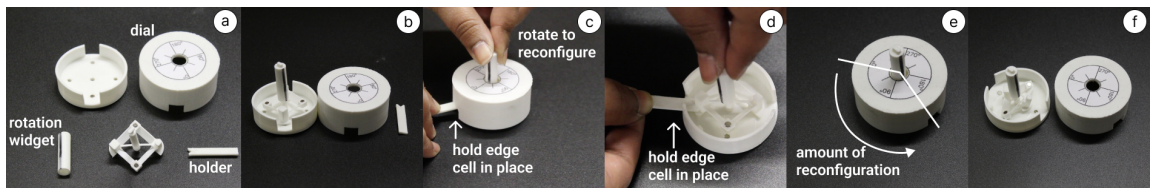


Fig. 18. Using rotation widget for reconfiguration through rotation of center pole

For the reconfiguration motion that requires rotation of the center pole on heating, a designer can use a dial based on the amount of reconfiguration required. In Figure 18, we have used a dial with degrees showing the amount of reconfiguration applied. Depending on the application, a high-level representation such as icons of increasing haptic feedback, or low-mid-high strength can also be used to assist end-user perception of reconfiguration range.

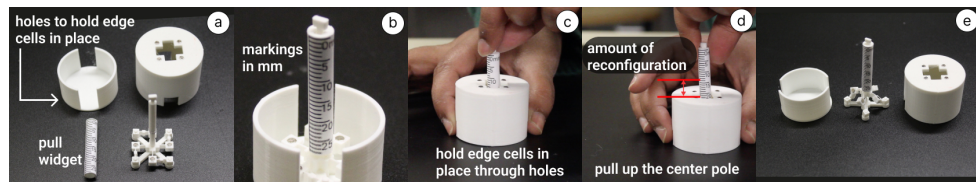


Fig. 19. Using pull widget for reconfiguration through pulling up of center pole

Similarly, for the reconfiguration motion requiring the pulling up of the center pole after heating the mechanism, the pole can have a widget cover indicating the length of the pole pulled up which can correspond to the expected deformation of the mechanism (Figure 19). Lastly, when pushing edge cells together for reconfiguration, a push widget that indicates how much the edge cell has been pushed in can give the user an idea of the expected feedback (Figure 20). These indicators can be ways of ensuring a specific type/amount of motion for reconfiguring a predefined amount of feedback. But, it is always possible for users to decide the amount of reconfiguration based on personal preferences.

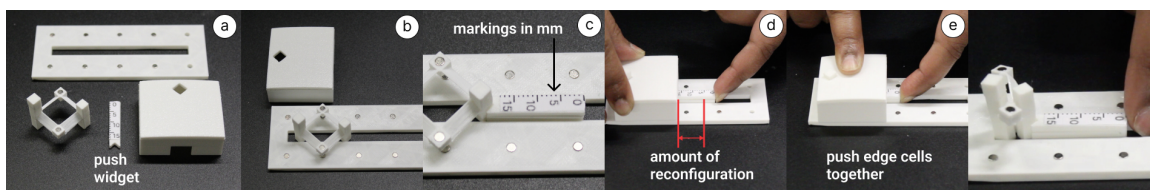


Fig. 20. Using push widget for reconfiguration through pushing edge cells together

625 5 EVALUATION OF RECONFIGURABLE INTERFACES

626 5.1 Understanding Shape Change and Displacement Relationships

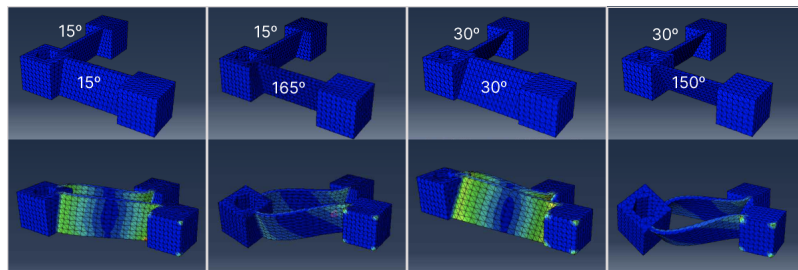
628 Related work has explored the control parameters of in/out-of-plane shape change to be hinge angles and their
 629 placements [22]. As we designed the geometry to work with heat-based shape change, and we are interested in
 630 displacement of the magnet cell through propagation of applied force, we first empirically validated that joint angles
 631 and lengths affect the magnet cell displacement.

633 To understand the relationships between joint angles and displacement, we printed a range of samples to gauge the
 634 relationships initially assessing parameter impact. We tested these samples by heating them in hot water and pushing
 635 the two edge cells together. We define joint angle θ as the angle made by the inner edge of the joint with respect to the
 636 vertical Z axis (refer Figure 2). From these samples, it was concluded that

- 638 • for movement of the magnet cell in the X-Y plane without any changes in Z axis, the joint angles must be set to 0°.
- 639 • for movement of the magnet cell in the Z axis without any changes in the X-Y plane, the joint angles must be equal
- 640 • to twist the magnet cell in the 3D space, the joint angles must be opposite i.e. subtracted from 180°(for e.g. 45°-135°.)

642 We also found that varying the joint length for the same joint angle resulted in different displacements. While the
 643 empirical evaluation unveiled a relationship between the joint angles and type of displacement, to further evaluate
 644 the effect of these parameters on the *extent* of magnet cell displacement, we conducted physics-based simulations
 645 measuring the displacements.

647 *5.1.1 Apparatus and Procedure.* Abaqus/CAE software enables Finite Element Modeling, visualization of the analyses,
 648 and simulating model states based on material, force, and environment settings. The software allows to test material-
 649 specific responses using PLA as input, and provided information about its characteristics and the environment. Given
 650 the ability to control the environment temperature and where the activation forces are applied, simulating the shape
 651 change using Abaqus gives close to real life results without human influence, and hence was chosen as a validation
 652 method. Tensile modulus was set to 3600MPa following the prior work [30] for PLA as our chosen shape memory
 653 material. Since the glass transition temperature (T_g) of PLA is generally between 60–65°C, the simulated temperature
 654 for triggering shape change was set to 80°C ($> T_g$). Since the amount of force applied by a human may vary, we simulate
 655 the displacement of the edge cells. For simulating the shape change, we fixed one edge cell and displace the other edge
 656 cell towards the fixed cell in the X-Y plane.



661 Fig. 21. Representative simulations conducted in Abaqus

673 All angles between 0-180° at an interval of 15° were produced for testing. Based on the observation from preliminary
 674 testing, 12 samples were chosen for simulation (7 samples for equal angles, 5 samples for opposite angles) such that

they covered all the combinations of the desired equal and opposite angles (45° - 135° combination of angles is considered same as 135° - 45°). The displacements of the magnet cells along X, Y, and Z axes, as well as the angular displacement were calculated by measuring the vector coordinates at the magnet cell before and after shape change. Figure 21 shows some representative simulated shape changed models.

In the second part of the simulations, we also tested the effect of various joint lengths on the displacement in two contexts, (1) where $\theta_1 = \theta_2 = 45^\circ$ for displacement along Z axis, and (2) where $\theta_1 = 45^\circ$ and $\theta_2 = 135^\circ$ for angular displacement. Displacements for joint lengths 5 – 40mm with intervals of 5mm were tested.

5.1.2 Results. The evaluation experiments show the relationship of the joint angles and joint lengths of a primitive with the extent of displacement which we use in our application examples.

- When $\theta_1 = \theta_2 \neq 0^\circ$,
 - v_d increases with increasing θ (without affecting a_d) where $\theta < 60^\circ$ as a_d is prominent ($> 5^\circ$) beyond $\theta = 60^\circ$
 - v_d increases with increasing joint length(l)
- When $\theta_1 = 180^\circ - \theta_2, \theta_1 < \theta_2$,
 - a_d increases with increasing θ_1 (without affecting v_d) where $\theta < 60^\circ$ as v_d is prominent beyond $\theta = 60^\circ$

Graphs in Figure 22 show the results of the performed simulation tests.

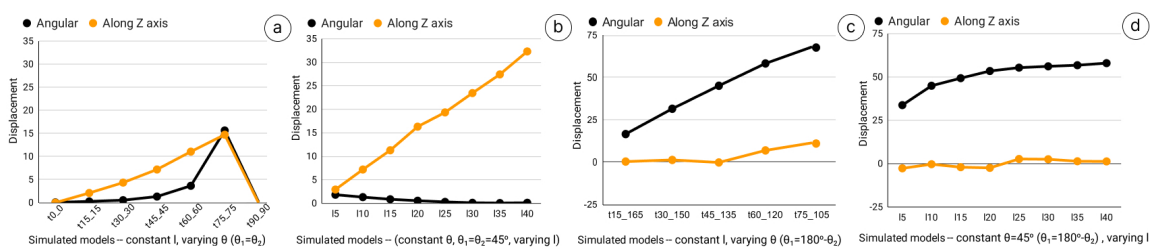


Fig. 22. Displacements for (a) constant joint length (l) and increasing $\theta_1 = \theta_2$, (b) constant joint angle ($\theta_1 = \theta_2 = 45^\circ$) and increasing joint lengths (l), (c) constant joint length (l) and increasing $\theta_1 = 180^\circ - \theta_2$, (d) constant joint angle ($\theta_1 = 45^\circ, \theta_2 = 135^\circ$) and increasing joint lengths (l).

#1. Increasing equal joint angles show increasing Z axis displacement. Displacement along Z axis in samples with constant length increases with increase in joint angle ($\theta_1 = \theta_2$) returning to 0mm at $\theta = 90^\circ$ (Figure 22(a)). However, we also see a certain amount of twisting or angular displacement as the angle increases. If we wish to control only the Z displacement, keeping the angular displacement to a minimum would be ideal i.e. in the range of 0-45°.

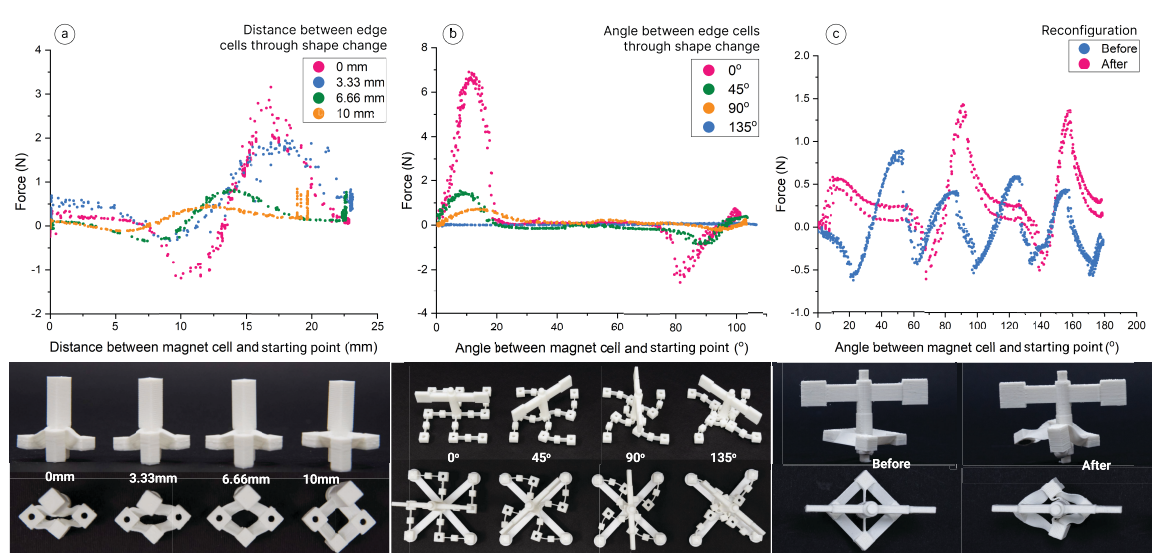
#2. For constant of equal joint angles, Z axis displacement can be increased by increasing joint length (l). On testing samples with $\theta_1 = \theta_2 = 45^\circ$ with increasing joint lengths (l5-l40), the Z displacement increased linearly (Figure 22(b)). Hence, beyond the joint angle, we can increase the Z displacement further by increasing the joint length.

#3. Increasing opposite joint angles show increasing angular displacement As seen from Figure 22(c), angular displacement increases with increase in θ_1 . But beyond $\theta_1 = 45^\circ$ ($\theta_2 = 180^\circ - \theta_1 = 135^\circ$), the graph shows an increase in Z displacement as well. Ideally if we only want to affect twisting, we would require the Z displacement to be negligible. Hence, we recommend joint angles to be used up to $\theta_1 = 45^\circ$.

#4. For constant opposite joint angles, angular displacement reaches a maxima with increasing joint lengths (l). As seen from Figure 22(d), while we see negligible Z displacement for increasing joint lengths (l5-l40), the angular displacement does not increase linearly, saturating at about 62°.

729 5.2 Understanding the Effect on Magnets

730 We validate the changes in the magnetic forces when the magnet cell is displaced by shape change. To test the effect
 731 of spatial displacement of magnets within the magnet cells with respect to a fixed magnet directly below them, we
 732 measured the force-distance curves for different edge cell displacements by constructing a rig. We used a dual-range
 733 force sensor coupled with a linear potentiometer to measure the distance between the magnet cell and the starting point.
 734 The force sensor pushes and pulls a 3D printed mechanism sample (square topology of the primitive geometry) hosting
 735 two magnets, along a rail with fixed magnets. Considering the maximum shape change to be 0mm distance between
 736 edge cells, we tested distances of 3.33mm, 6.66mm, and 10mm (no shape change). Figure 23 shows the tested samples,
 737 and the force-distance curves obtained. The Y axis shows the distance between the magnet cell and the starting point of
 738 the linear motion. The force-distance curve visualizes the haptic feedback during the relative movement of magnets.
 739 Since we used the attracting magnets, when magnets approach each other, the pulling force increases (negative value)
 740 reaching the minimal value; when magnets move away from each other, the pulling force increases (positive value)
 741 until it reaches the maximal value. From the four force-distance curves of edge cell displacement, we can observe a
 742 clear difference in both maximum and minimum force values for each curve, where the 0mm displacement has the
 743 highest difference between the maximum and minimum values, and 10mm has the smallest.
 744



745 Fig. 23. The force-distance/rotation curves obtained at various edge cell distances (a – top), reconfiguration angle (b – top) show that
 746 the force is proportional to the magnet cell's displacement. Changes in steps felt before and after de-activating a magnet cell (c – top).
 747 (a,b,c – bottom) show the corresponding samples used for measurement.

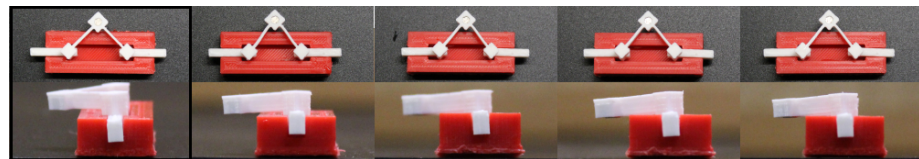
748 We measured the force-rotation curve for different horizontal displacements based on the spiral topology (Figure 6).
 749 We used the same dual-range force sensor coupled with a rotary potentiometer. The force sensor pushed a 3D-printed
 750 spiral topology sample hosting four magnets, along a round base with four embedded magnets. Considering the
 751 maximum shape change to be 135° rotation of the center pole, we tested other angles of 90°, 45°, and 0°(no shape change)
 752 as shown in Figure 23(b). The force-rotation curve visualized the haptic feedback during the relative movement of
 753 magnets. We can observe a clear difference in both maximum and minimum force values for each curve, where the
 754

781 0°sample has the highest pulling force during the rotation motion of the sample, while the 135°rotated sample has the
 782 smallest pulling force. The Y axis on the graph shows the angle between the magnet cell and the starting position.
 783

784 We also measured the force-rotation curve for angular displacements based on the square topology (Figure 12),
 785 visualizing the steps felt (resolution) during the relative movement of magnets. In the force curve of the switch where
 786 both magnet cells are in play, we can observe five times the peak and valley during the 180-degree rotation. While in
 787 the force curve of the switch where one of the magnet cells is deactivated, we can only observe two and a half times the
 788 peak and valley during the 180-degree rotation. The force-displacement/rotation curves showcase the different levels
 789 of resistance felt based on the applied amount of reconfiguration which can be utilized in applications such as the grip
 790 strengthener. The force is proportional to the displacement of the magnet cell from its original position. Hence, on
 791 scaling up the device geometry and using a proportionally larger magnet, the relationship between the feedback felt
 792 with the displacement of magnet cell from its original position should stay intact.
 793

794 5.3 Repeatability: Recovery Testing

795 As the forces are applied manually and the recovery expected is through shape memory, we also test the devices'
 796 sustainment through multiple cycles of reconfiguration. As studied in the prior work, "*with decreasing deformation*
 797 *temperature and increasing recovery temperature, both the shape-recovery ratio and the maximum shape-recovery rate of*
 798 *the PLA samples increased*", 90% recovery could be obtained [34]. Recovery ratio depends on the temperature at which
 799 the material is heated. As recovery attainable by 3D printed PLA has been previously investigated, we test on two
 800 sets of three primitive samples, at 2 joint lengths (15mm, 25mm), and 3 joint angle combinations (0°–0°, 45°–45°, and
 801 45°–135°) to show that our mechanisms conform to the principle. Each primitive sample was heated, reconfigured by
 802 pushing edge cells together, cooled down, and then reheated for recovery for four cycles. As Figures 24– 26 show, the
 803 recovered shape is not exactly the same as the initial printed shape, however, the difference is minimal.
 804



805 Fig. 24. Recovery test over 4 cycles (the first is initial) and shape memory recovery of primitive with 0°joint angles.
 806



807 Fig. 25. Recovery test over 4 cycles (the first is initial) and shape memory recovery of primitive with 45°- 45°joint angles.
 808



809 Fig. 26. Recovery test over 4 cycles (the first is initial) and shape memory recovery of primitive with 45°- 135°joint angles.
 810

833 6 DISCUSSION, LIMITATIONS, AND FUTURE WORK**834 6.1 Human Intervention in Reconfigurable Interfaces**

835 Our techniques require human intervention in the form of activation forces. We believe that this level of intervention
836 may benefit humans by giving them the full power to customize the reconfiguration to their need. Reconfiguration is
837 context and preference driven. Just as a musical instrument is tuned to the preference and requirement of a musician, or
838 a replaceable shelf is moved by a shorter person to be able to reach the top, reconfiguration of interfaces is dependent on
839 the human using them and that makes human intervention necessary to an extent. Our presented applications reiterate
840 the contextual nature of reconfiguration where it may be needed based on humans' ability, need for communication in
841 specific situations, safety, or simply a game's user experience.

842 6.2 Promoting Embodied Interaction with Physical Interfaces

843 While digital interfaces are overshadowing tangible interfaces in recent times, we cannot discount the use of tangibility
844 when it comes to multi-modal interactions. When users' visual capabilities are contextually impaired, for example,
845 while driving, or while being immersed in a VR environment, tangible and haptic interfaces provide the much needed
846 information for both safety and embodied experience. We see the potential of haptic feedback and tactility in addressing
847 accessibility concerns with visual or physical impairments (Figure 15), complementing digital interfaces, for rehabilitation
848 devices as shown in Figure 10), as well as for development of motor skills.

849 6.3 Other shape changing mechanisms

850 We only focus on manual shape change and recovery using shape memory in this work. While programmable shape
851 change allows self-assembly to a pre-programmed shape when the printed artifact is triggered by heat, this technique
852 utilizes the conflicting forces of shrinking caused by stresses released by the polymer in the direction of printed lines.
853 Such artifacts cannot be "unshrunk" even after re-heating and the changes in the size would need to be accounted for
854 in the design especially when embedding external objects such as magnets.

855 6.4 Further Evaluation and Design Assistance

856 We evaluated the relationship of joint angle and joint length with the displacement of the magnet cell. There are further
857 geometric parameters such as the angle between joints and the joint thickness contributing to the extent of displacement
858 and speed of recovery, and need to be evaluated. The relationship between different parameters can help in making
859 design decisions for example, where higher displacement may be needed in constrained spatial conditions, or where
860 vertical displacement might not be feasible and angular displacement might be the solution. The mechanisms created
861 in this work mostly are in $3mm \times 3mm$ or $6mm \times 3mm$ neodymium magnets. For higher magnetic forces and in larger
862 devices, stronger magnets might be necessary. The relationship of these parameters can be utilized in an editor for
863 assisting designers in creating similar mechanisms in their applications with input on the type of behavior expected.

864 7 CONCLUSION

865 We present reconfigurable interfaces, leveraging the shape-changing capabilities of 3D printed PLA and embedded
866 magnets. Using displacement of embedded magnets when triggered by shape change, various applications demonstrate
867 changing haptic feedback, and reconfigurable input motion to afford different interactions. We contribute techniques to
868 create reconfigurable interfaces where added efforts in part replacement or refabrication can be circumvented.

REFERENCES

- [1] Byoungkwon An, Ye Tao, Jianzhe Gu, Tingyu Cheng, Xiang'Anthony' Chen, Xiaoxiao Zhang, Wei Zhao, Youngwook Do, Shigeo Takahashi, Hsiang-Yun Wu, et al. 2018. Thermorph: Democratizing 4D printing of self-folding materials and interfaces. In *Proceedings of the 2018 CHI conference on human factors in computing systems*. 1–12.
- [2] Andrea Bianchi and Ian Oakley. 2013. Designing Tangible Magnetic Appcessories. In *Proceedings of the 7th International Conference on Tangible, Embedded and Embodied Interaction* (Barcelona, Spain) (*TEI '13*). Association for Computing Machinery, New York, NY, USA, 255–258. <https://doi.org/10.1145/2460625.2460667>
- [3] Xiang 'Anthony' Chen, Jeeeon Kim, Jennifer Mankoff, Tovi Grossman, Stelian Coros, and Scott E. Hudson. 2016. Reprise: A Design Tool for Specifying, Generating, and Customizing 3D Printable Adaptations on Everyday Objects. In *Proceedings of the 29th Annual Symposium on User Interface Software and Technology* (Tokyo, Japan) (*UIST '16*). Association for Computing Machinery, New York, NY, USA, 29–39. <https://doi.org/10.1145/2984511.2984512>
- [4] Scott Davidoff, Nicolas Villar, Alex S. Taylor, and Shahram Izadi. 2011. Mechanical Hijacking: How Robots Can Accelerate UbiComp Deployments. In *Proceedings of the 13th International Conference on Ubiquitous Computing* (Beijing, China) (*UbiComp '11*). Association for Computing Machinery, New York, NY, USA, 267–270. <https://doi.org/10.1145/2030112.2030148>
- [5] Sean Follmer, Daniel Leithinger, Alex Olwal, Akimitsu Hogge, and Hiroshi Ishii. 2013. InFORM: Dynamic Physical Affordances and Constraints through Shape and Object Actuation. In *Proceedings of the 26th Annual ACM Symposium on User Interface Software and Technology* (St. Andrews, Scotland, United Kingdom) (*UIST '13*). Association for Computing Machinery, New York, NY, USA, 417–426. <https://doi.org/10.1145/2501988.2502032>
- [6] Freddie Hong, Connor Myant, and David E Boyle. 2021. Thermoformed Circuit Boards: Fabrication of Highly Conductive Freeform 3D Printed Circuit Boards with Heat Bending. In *Proceedings of the 2021 CHI Conference on Human Factors in Computing Systems* (Yokohama, Japan) (*CHI '21*). Association for Computing Machinery, New York, NY, USA, Article 669, 10 pages. <https://doi.org/10.1145/3411764.3445469>
- [7] Alexandra Ion, Johannes Froehhofen, Ludwig Wall, Robert Kovacs, Mirela Alistar, Jack Lindsay, Pedro Lopes, Hsiang-Ting Chen, and Patrick Baudisch. 2016. Metamaterial mechanisms. In *Proceedings of the 29th annual symposium on user interface software and technology*. 529–539.
- [8] Mads Vedel Jensen, Jacob Buur, and Tom Djajadiningrat. 2005. Designing the User Actions in Tangible Interaction. In *Proceedings of the 4th Decennial Conference on Critical Computing: Between Sense and Sensibility* (Aarhus, Denmark) (*CC '05*). Association for Computing Machinery, New York, NY, USA, 9–18. <https://doi.org/10.1145/1094562.1094565>
- [9] Hyunyoung Kim, Céline Coutrix, and Anne Roudaut. 2018. KnobSlider: design of a shape-changing UI for parameter control. In *Proceedings of the 2018 CHI Conference on Human Factors in Computing Systems*. 1–13.
- [10] Donghyeon Ko, Jee Bin Yim, Yujin Lee, Jaehoon Pyun, and Woohun Lee. 2021. Designing Metamaterial Cells to Enrich Thermoforming 3D Printed Object for Post-Print Modification. In *Proceedings of the 2021 CHI Conference on Human Factors in Computing Systems* (Yokohama, Japan) (*CHI '21*). Association for Computing Machinery, New York, NY, USA, Article 671, 12 pages. <https://doi.org/10.1145/3411764.3445229>
- [11] Xiao Kuang, Devin J. Roach, Jiangtao Wu, Craig M. Hamel, Zhen Ding, Tiejun Wang, Martin L. Dunn, and Hang Jerry Qi. 2019. Advances in 4D Printing: Materials and Applications. *Advanced Functional Materials* 29, 2 (2019), 1805290. <https://doi.org/10.1002/adfm.201805290> arXiv:<https://onlinelibrary.wiley.com/doi/pdf/10.1002/adfm.201805290>
- [12] Thomas Langerak, Juan José Zárate, David Lindlbauer, Christian Holz, and Otmar Hilliges. 2020. Omni: Volumetric Sensing and Actuation of Passive Magnetic Tools for Dynamic Haptic Feedback. In *Proceedings of the 33rd Annual ACM Symposium on User Interface Software and Technology* (Virtual Event, USA) (*UIST '20*). Association for Computing Machinery, New York, NY, USA, 594–606. <https://doi.org/10.1145/3379337.3415589>
- [13] Jiahao Li, Jeeeon Kim, and Xiang 'Anthony' Chen. 2019. Robot: A Design Tool for Actuating Everyday Objects with Automatically Generated 3D Printable Mechanisms. In *Proceedings of the 32nd Annual ACM Symposium on User Interface Software and Technology* (New Orleans, LA, USA) (*UIST '19*). Association for Computing Machinery, New York, NY, USA, 673–685. <https://doi.org/10.1145/3332165.3347894>
- [14] Rong-Hao Liang, Liwei Chan, Hung-Yu Tseng, Han-Chih Kuo, Da-Yuan Huang, De-Nian Yang, and Bing-Yu Chen. 2014. GaussBricks: Magnetic Building Blocks for Constructive Tangible Interactions on Portable Displays. In *Proceedings of the SIGCHI Conference on Human Factors in Computing Systems* (Toronto, Ontario, Canada) (*CHI '14*). Association for Computing Machinery, New York, NY, USA, 3153–3162. <https://doi.org/10.1145/2556288.2557105>
- [15] Rong-Hao Liang, Han-Chih Kuo, Liwei Chan, De-Nian Yang, and Bing-Yu Chen. 2014. GaussStones: Shielded Magnetic Tangibles for Multi-Token Interactions on Portable Displays. In *Proceedings of the 27th Annual ACM Symposium on User Interface Software and Technology* (Honolulu, Hawaii, USA) (*UIST '14*). Association for Computing Machinery, New York, NY, USA, 365–372. <https://doi.org/10.1145/2642918.2647384>
- [16] Alex Mazursky, Shan-Yuan Teng, Romain Nith, and Pedro Lopes. 2021. MagnetIO: Passive yet interactive soft haptic patches anywhere. In *Proceedings of the 2021 CHI Conference on Human Factors in Computing Systems*. 1–15.
- [17] Jess McIntosh, Paul Strohmeier, Jarrod Knibbe, Sebastian Boring, and Kasper Hornbæk. 2019. Magnetips: Combining Fingertip Tracking and Haptic Feedback for Around-Device Interaction. In *Proceedings of the 2019 CHI Conference on Human Factors in Computing Systems* (Glasgow, Scotland UK) (*CHI '19*). Association for Computing Machinery, New York, NY, USA, 1–12. <https://doi.org/10.1145/3290605.3300638>
- [18] Kongpyung Moon, Haeun Lee, Jeeeon Kim, and Andrea Bianchi. 2022. ShrinkCells: Localized and Sequential Shape-Changing Actuation of 3D-Printed Objects via Selective Heating. In *Proceedings of the 35th Annual ACM Symposium on User Interface Software and Technology*. 1–12.
- [19] Ken Nakagaki, Artem Dementyev, Sean Follmer, Joseph A Paradiso, and Hiroshi Ishii. 2016. ChainFORM: a linear integrated modular hardware system for shape changing interfaces. In *Proceedings of the 29th Annual Symposium on User Interface Software and Technology*. 87–96.

- [20] Ken Nakagaki, Sean Follmer, and Hiroshi Ishii. 2015. Lineform: Actuated curve interfaces for display, interaction, and constraint. In *Proceedings of the 28th Annual ACM Symposium on User Interface Software & Technology*. 333–339.
- [21] Masa Ogata. 2018. Magneto-Haptics: Embedding Magnetic Force Feedback for Physical Interactions. In *Proceedings of the 31st Annual ACM Symposium on User Interface Software and Technology* (Berlin, Germany) (*UIST '18*). Association for Computing Machinery, New York, NY, USA, 737–743. <https://doi.org/10.1145/3242587.3242615>
- [22] Jifei Ou, Zhao Ma, Jannik Peters, Sen Dai, Nikolaos Vlavianos, and Hiroshi Ishii. 2018. KinetiX-designing auxetic-inspired deformable material structures. *Computers & Graphics* 75 (2018), 72–81.
- [23] Fang Qin, Huai-Yu Cheng, Rachel Sneeringer, Maria Vlachostergiou, Sampada Acharya, Haolin Liu, Carmel Majidi, Mohammad Islam, and Lining Yao. 2021. ExoForm: Shape Memory and Self-Fusing Semi-Rigid Wearables. In *Extended Abstracts of the 2021 CHI Conference on Human Factors in Computing Systems*. 1–8.
- [24] Raf Ramakers, Fraser Anderson, Tovi Grossman, and George Fitzmaurice. 2016. RetroFab: A Design Tool for Retrofitting Physical Interfaces Using Actuators, Sensors and 3D Printing. In *Proceedings of the 2016 CHI Conference on Human Factors in Computing Systems* (San Jose, California, USA) (*CHI '16*). Association for Computing Machinery, New York, NY, USA, 409–419. <https://doi.org/10.1145/2858036.2858485>
- [25] Joon Gi Shin, Doheon Kim, Chaehan So, and Daniel Saakes. 2020. Body Follows Eye: Unobtrusive Posture Manipulation Through a Dynamic Content Position in Virtual Reality. In *Proceedings of the 2020 CHI Conference on Human Factors in Computing Systems* (Honolulu, HI, USA) (*CHI '20*). Association for Computing Machinery, New York, NY, USA, 1–14. <https://doi.org/10.1145/3313831.3376794>
- [26] Joon-Gi Shin, Eiji Onchi, Maria Jose Reyes, Junbong Song, Uichin Lee, Seung-Hee Lee, and Daniel Saakes. 2019. Slow Robots for Unobtrusive Posture Correction. In *Proceedings of the 2019 CHI Conference on Human Factors in Computing Systems* (Glasgow, Scotland UK) (*CHI '19*). Association for Computing Machinery, New York, NY, USA, 1–10. <https://doi.org/10.1145/3290605.3300843>
- [27] Jihoon Suh, Wooshik Kim, and Andrea Bianchi. 2017. Button+ Supporting User and Context Aware Interaction through Shape-Changing Interfaces. In *Proceedings of the Eleventh International Conference on Tangible, Embedded, and Embodied Interaction*. 261–268.
- [28] Lingyun Sun, Jiaji Li, Yu Chen, Yue Yang, Ye Tao, Guanyun Wang, and Lining Yao. 2020. 4DTexture: A Shape-Changing Fabrication Method for 3D Surfaces with Texture. In *Extended Abstracts of the 2020 CHI Conference on Human Factors in Computing Systems* (Honolulu, HI, USA) (*CHI EA '20*). Association for Computing Machinery, New York, NY, USA, 1–7. <https://doi.org/10.1145/3334480.3383053>
- [29] Lingyun Sun, Yue Yang, Yu Chen, Jiaji Li, Danli Luo, Haolin Liu, Lining Yao, Ye Tao, and Guanyun Wang. 2021. ShrinCage: 4D Printing Accessories That Self-Adapt. In *Proceedings of the 2021 CHI Conference on Human Factors in Computing Systems* (Yokohama, Japan) (*CHI '21*). Association for Computing Machinery, New York, NY, USA, Article 433, 12 pages. <https://doi.org/10.1145/3411764.3445220>
- [30] J Antonio Travieso-Rodriguez, Ramon Jerez-Mesa, Jordi Llumà, Oriol Traver-Ramos, Giovanni Gomez-Gras, and Joan Josep Roa Rovira. 2019. Mechanical properties of 3D-printing polylactic acid parts subjected to bending stress and fatigue testing. *Materials* 12, 23 (2019), 3859.
- [31] Guanyun Wang, Ye Tao, Ozguc Bertug Capunaman, Humphrey Yang, and Lining Yao. 2019. A-line: 4D printing morphing linear composite structures. In *Proceedings of the 2019 CHI Conference on Human Factors in Computing Systems*. 1–12.
- [32] Guanyun Wang, Humphrey Yang, Zeyu Yan, Nurcan Gecer Ulu, Ye Tao, Jianzhe Gu, Levent Burak Kara, and Lining Yao. 2018. 4DMesh: 4D Printing Morphing Non-Developable Mesh Surfaces. In *Proceedings of the 31st Annual ACM Symposium on User Interface Software and Technology* (Berlin, Germany) (*UIST '18*). Association for Computing Machinery, New York, NY, USA, 623–635. <https://doi.org/10.1145/3242587.3242625>
- [33] Malte Weiss, Florian Schwarz, Simon Jakubowski, and Jan Borchers. 2010. Madgets: Actuating Widgets on Interactive Tabletops. In *Proceedings of the 23rd Annual ACM Symposium on User Interface Software and Technology* (New York, New York, USA) (*UIST '10*). Association for Computing Machinery, New York, NY, USA, 293–302. <https://doi.org/10.1145/1866029.1866070>
- [34] Wenzheng Wu, Wenli Ye, Zichao Wu, Peng Geng, Yulei Wang, and Ji Zhao. 2017. Influence of Layer Thickness, Raster Angle, Deformation Temperature and Recovery Temperature on the Shape-Memory Effect of 3D-Printed Polylactic Acid Samples. *Materials* 10, 8 (Aug. 2017), 970. <https://doi.org/10.3390/ma10080970>
- [35] Humphrey Yang, Tate Johnson, Ke Zhong, Dinesh Patel, Gina Olson, Carmel Majidi, Mohammad Islam, and Lining Yao. 2022. ReCompFig: Designing Dynamically Reconfigurable Kinematic Devices Using Compliant Mechanisms and Tensioning Cables. In *Proceedings of the 2022 CHI Conference on Human Factors in Computing Systems* (<conf-loc>, <city>New Orleans</city>, <state>LA</state>, <country>USA</country>, </conf-loc>) (*CHI '22*). Association for Computing Machinery, New York, NY, USA, Article 170, 14 pages. <https://doi.org/10.1145/3491102.3502065>
- [36] Clement Zheng, Jeeeon Kim, Daniel Leithinger, Mark D Gross, and Ellen Yi-Luen Do. 2019. Mechamagnets: Designing and fabricating haptic and functional physical inputs with embedded magnets. In *Proceedings of the Thirteenth International Conference on Tangible, Embedded, and Embodied Interaction*. 325–334.
- [37] Clement Zheng, Zhen Zhou Yong, Hongnan Lin, HyunJoo Oh, and Ching Chiuan Yen. 2022. Shape-Haptics: Planar & Passive Force Feedback Mechanisms for Physical Interfaces. In *Proceedings of the 2022 CHI Conference on Human Factors in Computing Systems*. 1–15.

Received 20 February 2007; revised 12 March 2009; accepted 5 June 2009